Scale-up of a single-mode microwave reactor

Himanshu Goyal[1], Ali Mehdad[1,2], Raul F. Lobo[1,2], Georgios D. Stefanidis[3], Dionisios G. Vlachos[1,2]*

1. Delaware Energy Institute, University of Delaware, 221 Academy Street, Newark, Delaware 19716, United States
2. Department of Chemical and Biomolecular Engineering, University of Delaware, 150 Academy Street, Newark, Delaware 19716, United States
3. Department of Chemical Engineering, KU Leuven, Celestijnenlaan 200F, B-3001 Leuven, Belgium

Abstract

Widespread use of microwave technology requires quantitative scale-up models. Currently, microwave models are typical qualitative in nature. This work focuses on rendering models quantitative and elucidating the scale-up behavior of microwave heating using numerical simulations. A commonly used bench-scale microwave reactor from the CEM Corp. (CEM Discover® SP) is used for benchmarking. To enable quantitative modeling, microwave heating experiments are conducted and compared to COMSOL calculations to develop a calibration curve for the set point vs. the actually delivered microwave power. Using the validated computational model, microwave-heating of various liquids in a wide range of vial sizes is investigated. The computational study shows that during the scale-up, the volumetric power absorbed passes through a maximum, whereas the energy efficiency and heating uniformity exhibit strongly nonlinear behavior. This work introduces a way for quantitative microwave models and insights into the scale-up of commercial microwave reactors.

Keywords: Microwaves, heating, COMSOL, scale-up

1. Introduction

To ameliorate global warming caused by the increasing level of greenhouse gases, efforts are underway to develop and deploy clean and sustainable sources of energy.[1, 2] One such effort is the utilization of electricity, sustainably generated from solar and wind, in chemical industries. In this regard, microwaves are a promising technology to achieve process intensification due to rapid, volumetric, and selective heating as opposed to conventional heating. These unique abilities of microwave heating are summarized in several works, e.g.[3-14]

Despite its potential, microwave heating is far from being implemented in chemical industry. The current fundamental understanding of microwave reactors is limited even at the lab-scale.[15] Several outcomes, such as the heating rate, temperature uniformity within the material, and energy efficiency, determine the effectiveness of microwaves and vary during scale-up in a poorly understood way. Difficulties associated with accurate measurements inside microwave reactors further exacerbate this situation. For instance, thermocouples cannot be employed for temperature measurement in the presence of an electromagnetic field and direct particle temperature measurement in multiphase systems is infeasible.

Despite experimental challenges, progress in commercial software, such as the COMSOL Multiphysics®[16], and computational resources allow detailed investigation of microwave heating in complex reactor geometries. Computational modeling, along with accurate experimental measurements, can significantly enhance our understanding of microwave-assisted chemical transformations as well as provide a platform for designing, optimizing, and scale-up of microwave reactors. Predictive modeling of microwave reactors is challenging though due to their resonant nature, i.e., microwaves form a standing wave within the reactor cavity where

microwave heating takes place. The spatial distribution of the microwave field is sensitive to materials properties, such as particle size and shape and dielectric constants.[17] For this reason, the present computational models for microwave reactors are qualitative in nature.[3, 17-20] Consequently, there is a strong need to improve their predictive abilities.

To remedy the above limitations, our first goal is to develop a predictive computational model for a commonly used bench-scale microwave reactor from CEM Corp. (CEM Discover® SP[16]) and validate the model against experiments. To expedite the widespread use of microwave reactors, a better understanding of scale-up is required. In the literature, there have been a few scale-up studies for microwave heating of liquid and solid batch systems.[19, 21, 22] However, a detailed picture of the underlying phenomena is still missing. Our second goal is to investigate the scale-up of microwave heating of liquid batch systems in the CEM Discover® SP reactor.

2. Computational Model

2.1 Governing Equations

This section describes the mathematical equations governing the phenomena of microwave heating: the spatial distribution of electromagnetic (EM) field inside the microwave reactor and the heating of the dielectric material due to the electromagnetic energy dissipation. For time-harmonic or sinusoidal EM waves in a source-free, linear, isotropic, and homogeneous medium, Maxwell's equations can be transformed into a simpler form known as the wave equation or Helmholtz equation given by[23]:

$$\nabla^2 \boldsymbol{E} + k^2 \boldsymbol{E} = 0$$

$$\nabla^2 \boldsymbol{H} + k^2 \boldsymbol{H} = 0 \qquad (1)$$

Here, $\boldsymbol{E}$ and $\boldsymbol{H}$ are the electric and magnetic fields, respectively in the phasor form. $k = \omega\sqrt{\mu\varepsilon}$ is the propagation constant, ω is the angular frequency, and ε and μ are the complex permittivity and permeability of the medium, respectively. It is convenient to use the relative permittivity, $\varepsilon_r = \varepsilon/\varepsilon_0 = \varepsilon' - j\,\varepsilon''$, and the relative permeability, $\mu_r = \mu/\mu_0 = \mu' - j\mu''$, with $\varepsilon_0 = 8.854 \times 10^{-12}$ F/m and $\mu_0 = 4\pi \times 10^{-7}$ H/m being the permittivity and permeability of the free space, respectively. The materials considered here have $\mu_r = 1$. Another important quantity is the loss tangent tanδ defined as:

$$tan\delta = \frac{\varepsilon''}{\varepsilon'}. \qquad (2)$$

tanδ quantifies the ability of a material to be heated in a microwave field. Higher values of tanδ are associated with a higher propensity towards microwave heating.

The tangential components of the electric and magnetic fields are continuous across an interface between two mediums with no charge or surface current density and can be written as[23]:

$$\hat{\boldsymbol{n}} \times \boldsymbol{E_1} = \hat{\boldsymbol{n}} \times \boldsymbol{E_2}$$

$$\hat{\boldsymbol{n}} \times \boldsymbol{H_1} = \hat{\boldsymbol{n}} \times \boldsymbol{H_2}, \qquad (3)$$

where $\hat{\boldsymbol{n}}$ is the unit normal vector at the interface between medium 1 and 2. $\boldsymbol{E_1}$and $\boldsymbol{E_2}$ are the electric fields in medium 1 and 2, respectively, whereas $\boldsymbol{H_1}$and $\boldsymbol{H_2}$ are the magnetic fields in medium 1 and 2, respectively. The metallic walls of the reactor are assumed to be perfect conductors making all the components of the electric and magnetic fields inside the conducting region zero[23]:

$$\hat{\boldsymbol{n}} \times \boldsymbol{E} = 0$$

$$\hat{\boldsymbol{n}} \times \boldsymbol{H} = 0. \qquad (4)$$

At the inlet port, a transverse electric mode, TE_{10}, is established.

The temperature profile of the material being heated in a microwave field can be evaluated by solving the energy balance equation:

$$\rho C_p \frac{\partial T}{\partial t} + \rho C_p \boldsymbol{u}.\nabla T = -\nabla.(\kappa \nabla T) + \rho_p \,, \qquad (5)$$

where ρ, C_p, and κ are the mass density, specific heat capacity, and thermal conductivity of the medium, respectively. T and $\boldsymbol{u}$ are the temperature and velocity at a given point inside the medium. The volumetric power absorbed ρ_p in a medium due to the electromagnetic energy dissipation is given by:

$$\rho_p = \frac{1}{2}\omega \varepsilon_0 \varepsilon'' |\boldsymbol{E}|^2 \qquad (6)$$

where $|\boldsymbol{E}|$ represents the magnitude of $\boldsymbol{E}$.

Evaluation of the spatial temperature profile in a fluid medium requires the knowledge of $\boldsymbol{u}$ for which the Navier-Stokes equation and the continuity equation need to be solved along with Eqs. (1) and (5). The experiments performed in this work achieve a uniform temperature within the liquids during the microwave heating using magnetic stirring. Therefore, in the computational model, the knowledge of the actual flow field is not required. Instead, a sufficiently high value of κ is used in Eq. (5) to obtain a uniform temperature field within the liquid. This simplification has previously been used in the literature.[18] It should be noted that for large batch and multiphase systems, such as a slurry reactor, there can be temperature gradients within the reactor and a full flow field will then be required to predict the temperature field. Adiabatic boundary condition

is applied at the outside boundary of the vial, whereas at the interface of two mediums thermal equilibrium is assumed.

The governing equations along with the appropriate boundary conditions are solved in the COMSOL Multiphysics® software,[24] referred to as COMSOL. The RF module and the Heat Transfer module are employed. These modules allow to perform transient three-dimensional simulations of microwave heating. The temperature dependence of the dielectric property makes Eqs. (1) and (5) two-way coupled. A change in the dielectric property of a material modifies the EM field distribution inside the reactor cavity, which in turn affects the power absorbed within the material. More details about the workings of the relevant COMSOL modules can be found in Ref.[17] As there is a large separation between the time scales associated with EM waves, $\mathcal{O}(10^{-9}$ s), and the heating of a material, $\mathcal{O}(10^{1}$ s), COMSOL updates the EM field periodically rather than at every single time step during the transient simulations. COMSOL utilizes the finite element method to obtain a numerical solution of the governing equations.

For the model calibration and validation studies, transient simulations are performed using the *Frequency-Transient* study type in COMSOL, whereas for the scale-up study, non-transient simulations are performed using the *Frequency-Domain* study type. A mesh independence study is conducted for the smallest (inner vial diameter of 0.5 mm) and the largest vial (inner vial diameter of 30 mm) considered in this work. *Frequency-Domain* simulations are performed by varying the *Physics-controlled Mesh* setting in COMSOL from “Extremely Coarse” to “Finer”. In these simulations water, ethanol, and hexane are included with a liquid height of 40 mm inside the vials. Values of two targets, namely the mean and variance of the power absorbed, are compared for different mesh settings. We found the “Fine” mesh setting of COMSOL to be

satisfactory as further mesh refinement changed the targets by less than 3% and 4% for the smallest and the largest vial, respectively. Therefore, *Physics-controlled Mesh* is set to "Fine" during all the COMSOL simulations. A typical number of mesh elements is about 10^5.

2.2 Simulation Setup

In this work, the CEM Discover® SP is used to develop a predictive microwave heating model and perform the scale-up study of liquid batch systems. The geometry of the reactor is built in COMSOL and is shown in Figure 1. For details about the geometry and working of the reactor, the reader is referred to refs.[17, 19, 25] A short description of the microwave reactor is presented here.

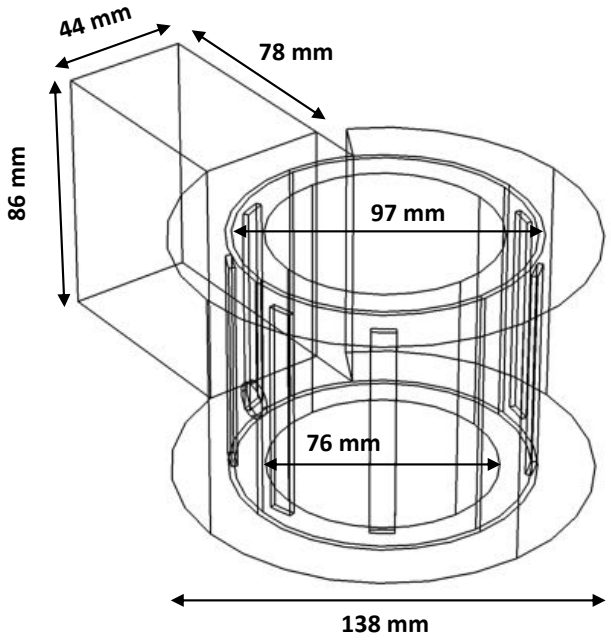

Figure 1. *Three-dimensional microwave reactor configuration built in COMSOL.*

2.3 Experiments

The specific microwave reactor utilizes a magnetron to generate microwaves with a power ranging from 1 W to 300 W at a frequency of 2.45 GHz. Microwaves generated by the magnetron are transmitted to a cylindrical cavity with the help of a waveguide. Six rectangular slots in the metal wall between the cylindrical cavity and the waveguide allow the exchange of EM waves between them. A vial containing a dielectric material is placed inside the cylindrical cavity. Fiber optics (FO) and Infrared (IR) pyrometer are used to measure the temperature in-situ and at the outer surface of the vial, respectively.

In the experiments, microwave heating of 2 ml and 4 ml of water, ethanol, and hexane in a 10 ml Pyrex vial is performed at input powers of 30 W, 100 W, 200 W, and 300 W in the CEM Discover® SP reactor. During the microwave heating, a magnetic stirrer is used to maintain a uniform temperature within the liquid being heated in the vial. A total of 24 distinct experiments are performed. Each experiment is repeated three times to obtain the standard deviation in the measurements. The experimental temperature profiles are provided in Figure S1 in the Supporting Information. Water, ethanol, and hexane are selected due to possessing dielectric properties spanning a wide range.

3. Model Assessment

To assess our model, the experiments of Robinson et al.[18] are simulated and our model predictions are compared with their COMSOL model predictions and their experimental measurements (Figure 2). The system entailed various liquids (3 mL in volume) in a 10 mL Pyrex vial in the CEM Discover® SP reactor using a microwave power of 30 W and fast magnetic stirring and a fiber optic for temperature measurements.

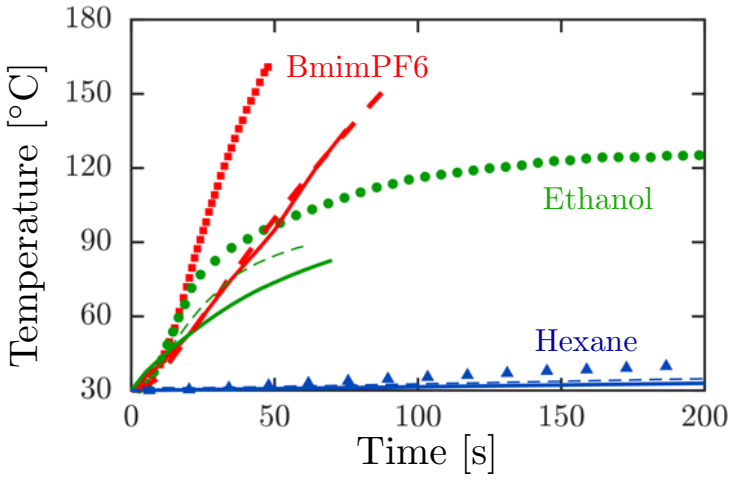

Figure 2. *Temperature profiles of liquids during microwave heating. Predicted temperature profiles from this work (solid lines) and experimental measurements (symbols) and model predictions (dashed lines) of Robinson et al.*[18]

Figure 2 compares the experimental temperature profiles from Ref.[18] of BMimPF6 (an ionic liquid), ethanol, and hexane to theirs and our simulations. Very good agreement between simulation predictions is seen but the simulations under-predict the experimental data. Sturm et al.[17, 19] have reached similar conclusions for microwave heating of water. As a second test case, our model predictions are compared against the experiments of Sturm et al.[19] for the total power absorbed P_{absorbed} normalized by the maximum, as shown in Figure 3. In their experiments, Sturm et al.[19] measured the power absorbed by water heated in borosilicate glass vials of varying diameters in the CEM Discover® SP microwave reactor. A constant liquid height of 40 mm and a microwave power of 300 W were used. The very good agreement between the simulations and the experiments in Figure 3 implies that the delivered microwave power differs from the specified power by a constant factor independent of the vial size. We discuss this point further below. A detailed analysis of the effect of the vial diameter on the power absorbed and other parameters is provided in Section 4.

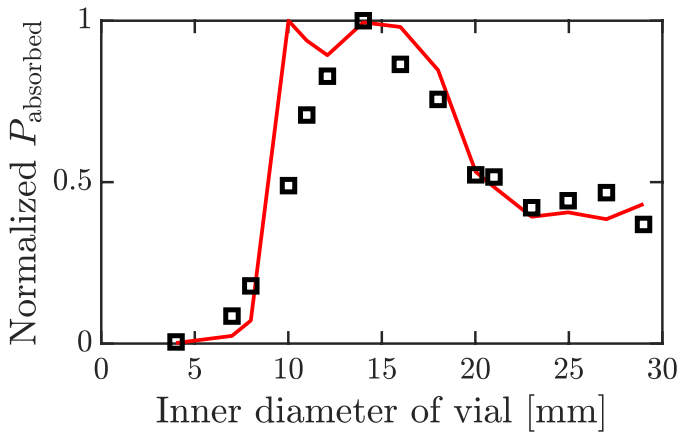

Figure 3. *Absorbed microwave power $P_{absorbed}$ [W] normalized by the maxima as a function of vial diameter. Comparison of the simulations (lines) and the experiments (symbols, from Ref.[19]).*

4. Calibration toward Quantitative Model Predictions

At present, simulations of microwave heating in the CEM Discover® SP reactor are only qualitative in nature.[3, 17-19] Based on several literature studies,[17, 19, 26] two major sources of uncertainty are identified: 1) the net power delivered by the microwave reactor and 2) the dielectric properties of materials. In the CEM Discover® SP reactor, the net power delivered by the magnetron to the load cannot be measured. Also, it is extremely difficult to compute as it would require an accurate model of the magnetron coupled with the applicator. Sturm et al.[17, 19] attempted to address this problem using an idealized lumped magnetron model. However, large deviations (>100%) from the experiments were observed.

The above-mentioned uncertainties need to be accounted for to render the model predictive. As a first step towards developing predictive modeling, a series of experiments and simulations are performed to obtain the optimal values of dielectric properties within their uncertainty limits and a calibration curve for the delivered microwave power corresponding to a specified input power (set point) is developed.

The values of ε_r and tanδ for the select liquids and Pyrex are obtained from refs.[17, 18, 27] and are provided in Table 1. Refs.[26, 28, 29] indicate that a conservative estimate for the uncertainty in ε' and ε'' is 2% and 5%, respectively. For the calibration, ε' and $\varepsilon''$are multiplied by constant factors f_1 and f_2, respectively, such that $\varepsilon_r = f_1\varepsilon' - jf_2\varepsilon''$. Sturm et al.[19] found that the delivered power can be higher than the power specified to the microwave reactor by a factor greater than two. In the calibration study, the power delivered P_{out} is allowed to vary from the specified input power, P_{in}, by a factor between 1 and 3. P_{out} is not let to be lower than P_{in} as several experimental studies have shown that $P_{\text{out}} > P_{\text{in}}$.

Table 1. Values of the relative permittivity and tanδ at 2.45 GHz frequency and 20 °C.

Material	Relative permittivity, $\boldsymbol{\varepsilon_r}$	tan$\boldsymbol{\delta}$
Water	78.0-j10.50	0.13
Ethanol	6.6-j6.30	0.95
Hexane	1.9-j0.0376	0.02
Pyrex	3.3-j0.026	0.008

The calibration is performed by minimizing the least square difference between the simulation predictions and the experiment data. With the above constraints, the following objective function is minimized to obtain the optimal values of f_1, f_2, and P_{out}:

$$\Phi(f_1^*, f_2^*, P_{out}^*) = \min\_f_1, f_2, P_{out} \sum_1^n \left(\frac{\mathcal{J}_i^{sim}(f_1, f_2, P_{out}) - \mathcal{J}_i^{exp}}{{\sigma_i}^{exp}} \right)^2 \qquad (7)$$

$$0.98 < f_1 < 1.02, 0.95 < f_2 < 1.05, P_{in} < P_{out} < 3\ P_{in}\ .$$

Here, f_1^*, f_2^*, and P_{out}^* are the optimal values of f_1, f_2, and P_{out}, respectively. i is the index of the experiment and the corresponding simulation, n is the total number of experiments, σ_i^{exp} is the standard deviation in the experimental measurement, and $\mathcal{J}_i^{sim}$ and $\mathcal{J}_i^{exp}$ are the simulation predictions and experimental measurements of the average heating rates of the liquid samples, respectively. $\mathcal{J}_i^{sim}$ and $\mathcal{J}_i^{exp}$ are calculated as:

$$\mathcal{J}_i^p = \frac{T_{final}^p - T_{initial}^p}{t_{final}^p - t_{initial}^p}, \qquad (8)$$

where the superscript p stands for either an experimental measurement or a simulation prediction. T_{final}^p is 10 °C lower than the boiling point of the liquid used, $T_{initial}^p$ is 25 °C (~5 °C above the room temperature). These values are selected to reduce the uncertainties present at the beginning of the experiments and near the boiling point of the liquids. t_{final}^p and $t_{initial}^p$ are the time values corresponding to T_{final}^p and $T_{initial}^p$, respectively. In the case of hexane, the heating rate is about two orders of magnitude lower than that of water and ethanol. Heat losses due to natural convection become significant during this experiment. For this reason, $T_{final}^p$is taken as 30 °C to minimize the impact of heat loss to the surrounding. To solve the optimization problem (Eq. (7)) in a computationally affordable manner, $\mathcal{J}_i^{sim}$ is represented by a response surface in the form of a second-order polynomial. The coefficients are calculated using regression, in which the values of f_1 and f_2 are determined using a factorial design.[30, 31] $\mathcal{J}_i^{sim}$ varies linearly with P_{out}, and therefore is not included in the factorial design. The created response surfaces are provided in Figure S2 in the Supporting Information.

Equation (7) is solved using MATLAB and the resulting optimal values of f_1 and f_2 are provided in Table 2. Figure 4 shows P_{out} as a function of P_{in} and clearly demonstrates that the percent

deviation of P_{out} from P_{in} increases as P_{in} decreases. A quadratic equation is fitted to provide P_{out} as a function of P_{in}:

$$P_{\text{out}}(\text{W}) = -0.0005\, P_{\text{in}}^2 \;+\; 1.0379\, P_{\text{in}} \;+\; 28.929, \text{P}_{\text{in}} \text{ in W}. \tag{9}$$

Table 2. Optimal values of f_1^* and f_2^* .

Solvent	f_1^*	f_2^*
Water	1.02	0.95
Ethanol	0.98	1.05
Hexane	1.02	0.95

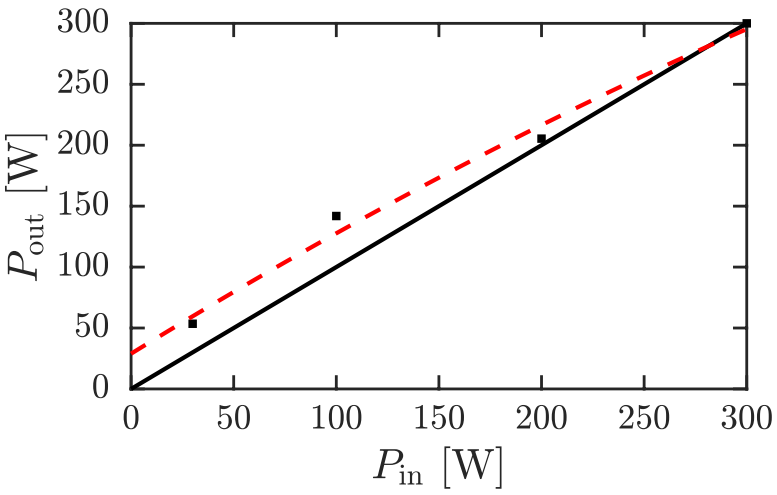

Figure 4. *Delivered microwave power P_{out} as a function of specified input power P_{in}. Symbols are the calculated values from Eq. (7). Dashed line is the fitted quadratic equation (Eq. (9)) with an R^2 value of 0.99.*

Using the developed power calibration curve and the estimated dielectric properties, the experiments of Robinson et al.[18] are simulated again, and the results are compared in Figure 5. Significant improvement in agreement, compared to Figure 2, is seen. BMimPF6 was not used in the calibration study and the volume of the liquid (3 ml) is also different from the calibration experiments. These results along with the very good agreement in Figure 3 shows that the delivered microwave power is independent of material type and quantity. Thus, the calibration curve can be used for other type and quantities of liquids in the CEM Discover® SP. The methodology introduced here to extract dielectric properties under relevant conditions and estimate the actual power delivered vs. the set point can be generalized to other systems of interest.

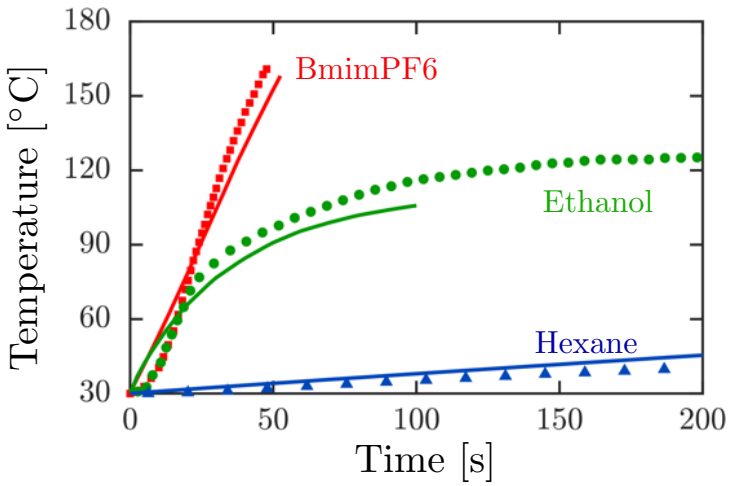

Figure 5. *Temperature profiles of liquids during microwave heating. Predicted temperature profiles using the calibration curve developed in this work (solid lines) vs. the experimental measurements (symbols) of Robinson et al.[18]*

5. Scale-up of Microwave Heating

The developed COMSOL model is employed to gain insights into the scale-up of microwave heating. Three quantities of interest (QoIs) are identified for this purpose: 1) volumetric power absorbed, 2) energy efficiency, and 3) uniformity of the power absorbed. The volumetric/specific power absorbed ρ_p is calculated using Eq. (6). The energy efficiency η of microwave heating is defined as

$$\eta = \frac{P_{\text{absorbed}}}{P_{\text{input}}}. \qquad (10)$$

Here, P_{absorbed} and P_{input} are the power absorbed by the load and the input power of the microwave reactor, respectively.

Uniformity of the distribution of ρ_p is quantified using the coefficient of variance (CV) defined as

$$CV = \frac{\sigma}{\mu}, \qquad (11)$$

where σ and μ are the standard deviation and the mean of ρ_p. The magnitude of CV is proportional to the non-uniformity in the distribution of ρ_p.

In general, the dielectric properties of materials change with temperature, and therefore, all the above mentioned QoIs can also change during the heating of a material. Due to lack of temperature dependent materials properties, we focus on the initial heating of various liquids initially at room temperature (20 ^{o}C) to elucidate the general behavior of microwave heating during scale-up. It should be noted that the knowledge of temperature-dependent dielectric properties becomes essential when the prediction of the transient temperature profiles is required. Currently, such data is not readily available.

For the scale-up study, microwave heating of water, ethanol, and hexane in Pyrex vials with a wide range of diameters is considered. The materials and geometric conditions used in the simulations are reported in Table 3. The minimum and maximum volume of the liquid samples correspond to 15.7 μL and 124.7 mL, respectively. Using the COMSOL model, non-transient *Frequency-Domain* simulations are performed and the EM field distribution inside the microwave reactor is calculated. In the Supporting Information, Figure S3 shows the distribution of the electric field norm inside the reactor cavity without any load and with a Pyrex vial filled with different liquids. With the knowledge of complete EM field, the QoIs are calculated using Eqs. (6), (10), and (11). Each QoI is investigated in the following subsections.

Table 3. Materials and geometric conditions used for the computational scale-up study.

Variable	Value
Material	Water, ethanol, hexane
Inner diameter of vial, d_{vial}	1 mm to 60 mm
Vial thickness	2 mm
Height of material in the vial, h_{liq}	20 mm and 40 mm
Microwave power	100 W

5.1. Power Absorbed

Figure 6 shows the variation of the mean power absorbed over the liquid volume $\bar{\rho}_p$ and the mean rate of change of temperature $\dot{T}$ as a function of the inner diameter of the vial d_{vial}. $\dot{T}$ is

calculated as $\bar{\rho}_p/\rho C_p$. Figure 6 shows that $\bar{\rho}_p$ and $\dot{T}$ first increase and then decrease with increasing d_{vial}. Two regimes are identified for the decrease of $\bar{\rho}_p$ and $\dot{T}$: a sharp drop (>90%) followed by a small gradual decrease and a possible second local maximum, with increasing d_{vial}. For ethanol and hexane, $\bar{\rho}_p$ decreases with increasing the liquid height, whereas for water, $\bar{\rho}_p$ increases with the liquid height for smaller d_{vial} and decreases for larger d_{vial}. The maximum value of $\bar{\rho}_p$ for water is higher than that of ethanol, even though ethanol has a much higher value of $\tan\delta$. This observation shows that $\tan\delta$ alone cannot be used to determine the heating ability of a material in a microwave reactor; both ε' and ε'' need to be considered. These observations are further analyzed in Figure 7.

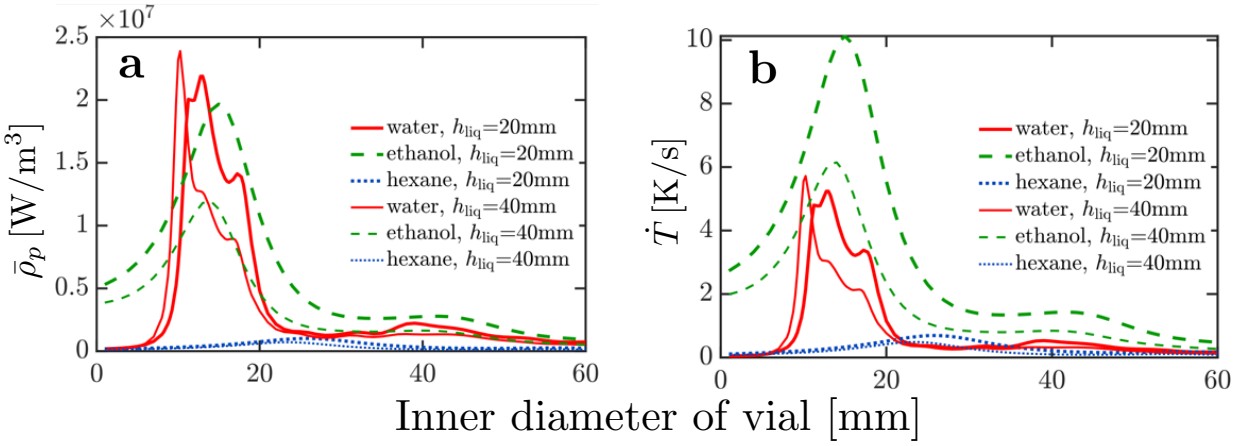

Figure 6. *(a) Mean volumetric power absorbed $\bar{\rho}_p$ (W/m³) as a function of d_{vial}. (b) Mean heating rate $\dot{T}$ (K/s) as a function of d_{vial}. Liquid height is equal to 20 mm or 40 mm.*

Figure 7a compares the values of $\bar{\rho}_p$ for all the liquids normalized by their maximum. There is a negligible impact of liquid height on the profiles, therefore, the data for only h_{liq}=40 mm is shown in Figure 7. It can be seen that as ε' increases ($\varepsilon'_{\text{water}} = 78, \varepsilon'_{\text{ethanol}} = 6.6, \varepsilon'_{\text{hexane}}$ =1.9), the width of the profile decreases and the peak shifts to a smaller d_{vial}. This observation implies that scale-up favors materials with lower ε', as the peak value of $\bar{\rho}_p$ can be achieved at larger vial sizes. Another important observation is that the normalized $\bar{\rho}_p$ approaches significantly different values as d_{vial} approaches zero. It is close to zero for water but is much higher for ethanol and hexane. These observations can be explained by the strong dependence of the EM field distribution on the quantity and type of the material present in the microwave reactor.

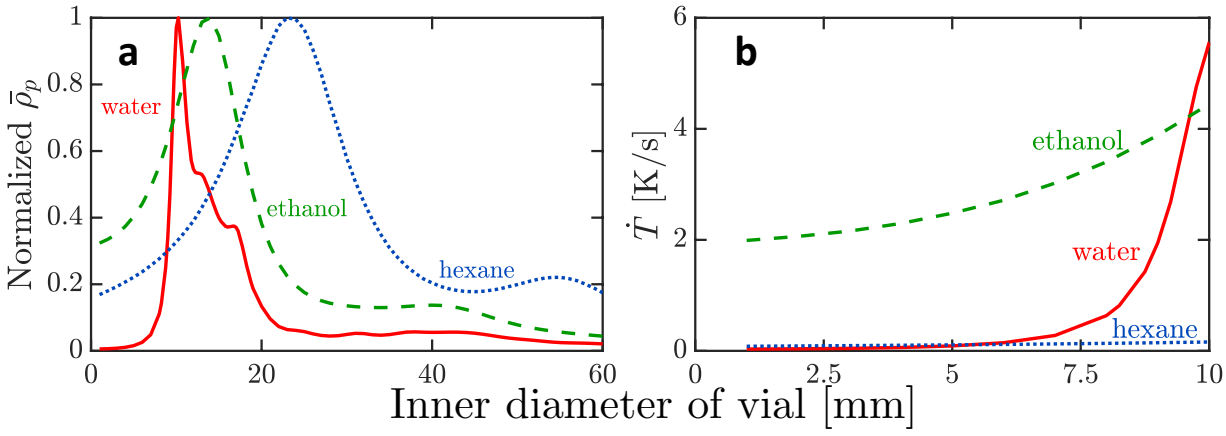

Figure 7. *(a) Normalized mean volumetric power absorbed as a function of d_{vial}. (b) Mean heating rate $\dot{T}$ (K/s) as a function of d_{vial}. Liquid height is equal to 40 mm.*

Figure 7b compares $\dot{T}$ for all the liquids for d_{vial} < 10 mm and shows that as d_{vial} approaches zero, there is a sharp decrease in the heating rate of water and it becomes smaller than the heating rate of hexane for d_{vial} < 6 mm. This observation implies that depending on the geometry

of the load, a strongly microwave absorbing material can exhibit lower heating compared to a weakly microwave absorbing material.

Interestingly, the standard Pyrex vial with 10 mL capacity provided by the CEM Corp. has d_{vial}=12 mm, which is close to the value of d_{vial} corresponding to the maxima of $\bar{\rho}_p$ and $\dot{T}$ for water, i.e., the design of the CEM Discover® SP microwave reactor has been optimized to heat water-based samples in a 10 mL Pyrex vial.

5.2 Energy Efficiency

The microwave heating efficiency η is an important factor in determining the potential benefits of microwaves. Figure 8 shows η, calculated using Eq. (10), for all the cases considered for the scale-up study. Two local efficiency peaks are observed for all the liquids. The first one is near d_{vial}, which maximizes $\bar{\rho}_p$, whereas the second one occurs at a much larger d_{vial}. These observations can be explained by considering that P_{absorbed} varies as $\bar{\rho}_p \times V_{\text{liquid}}$, where V_{liquid} is the volume of the load. Both the load and the EM field distribution within the load determine the energy efficiency. Therefore, even though $\bar{\rho}_p$ decreases after a certain vial size during the scale-up, η increases. Moreover, there is a negligible impact of the liquid height on the efficiency trend.

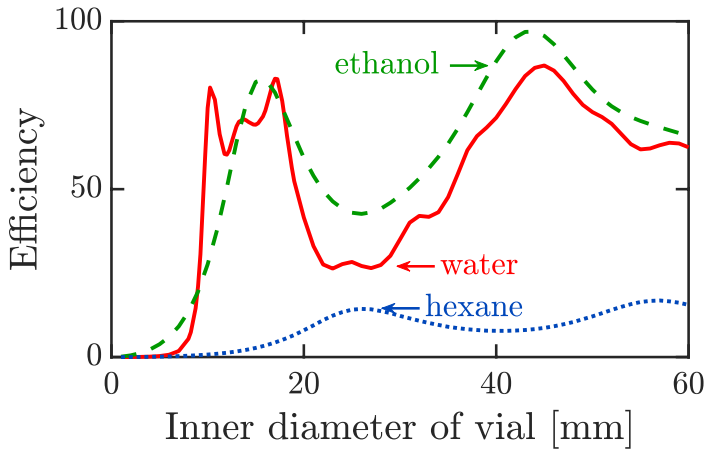

Figure 8. *Microwave heating efficiency η (percent) during scale-up. Variation of η as a function of d_{vial} for water, ethanol, and hexane. The liquid height is equal to 40 mm.*

Bermudez et al.[21] performed an extensive experimental scale-up study of microwave heating of different materials (both liquid and solid) in single-mode and multi-model microwave reactors. The trends observed in our computational study bear excellent agreement with those of their work. Two major observations are reported here: (1) A sharp decrease (90-95%) in the $\bar{\rho}_p$ followed by a gradual and moderate decrease during the scale-up. Figure 6 shows that after a certain vial size, $\bar{\rho}_p$ first drops significantly and then decreases gradually. (2) An non monotonic variation of η during the scale-up (Figure 8) with the second maximum being higher than the first one and exceeding 90%. These observations indicate that the general trend of scale-up in microwave reactors is independent of the load and the reactor type, but the actual values of the power absorbed and the energy efficiency vary with reactor design.

5.3 Uniformity of the Power Absorbed

A major problem with microwave heating is the highly non-uniform distribution of the microwave heat source within the load. To understand the distribution of absorbed power, the coefficient of variation CV is calculated for ρ_p using Eq. (11). Figure 9 shows the CV as a function of d_{vial}. Overall, the CV shows a highly non-monotonic behavior with increasing d_{vial} for all liquids. Figure 10 provides a visual representation of the distribution of ρ_p inside the liquids for d_{vial}=20 mm, 40 mm, and 60 mm. In the case of water, multiple peaks of ρ_p are observed for all the d_{vial}, whereas in the case of ethanol and hexane, ρ_p is maximum near the center for d_{vial}=20 mm and near the wall for d_{vial}=60 mm.

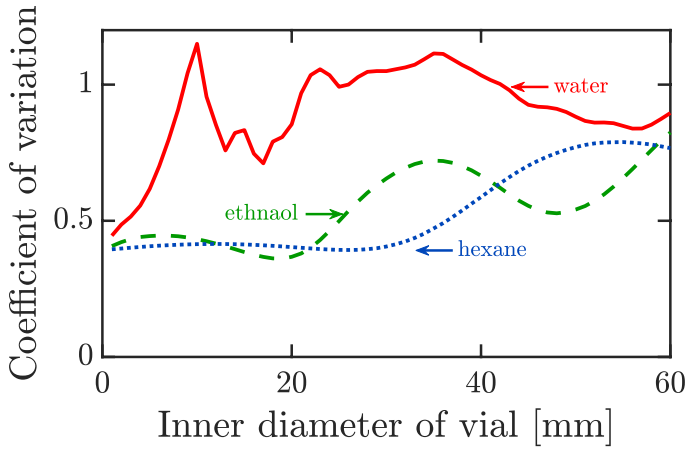

Figure 9. *Coefficient of variation CV for ρ_p during scale-up for water, ethanol, and hexane. The liquid height is equal to 40 mm.*

These observations point to the sensitive standing wave pattern of microwaves in the reactor cavity and the heating sample. When the sample is comparable to the wavelength of the EM wave, a wave pattern forms within the sample due to the interference of the incident wave and the wave reflected from the end surface.[32] The penetration depth D_p and the reflection

coefficient Γ are two important parameters that affect the wave pattern formed within the sample and hence the uniformity of microwave heating.

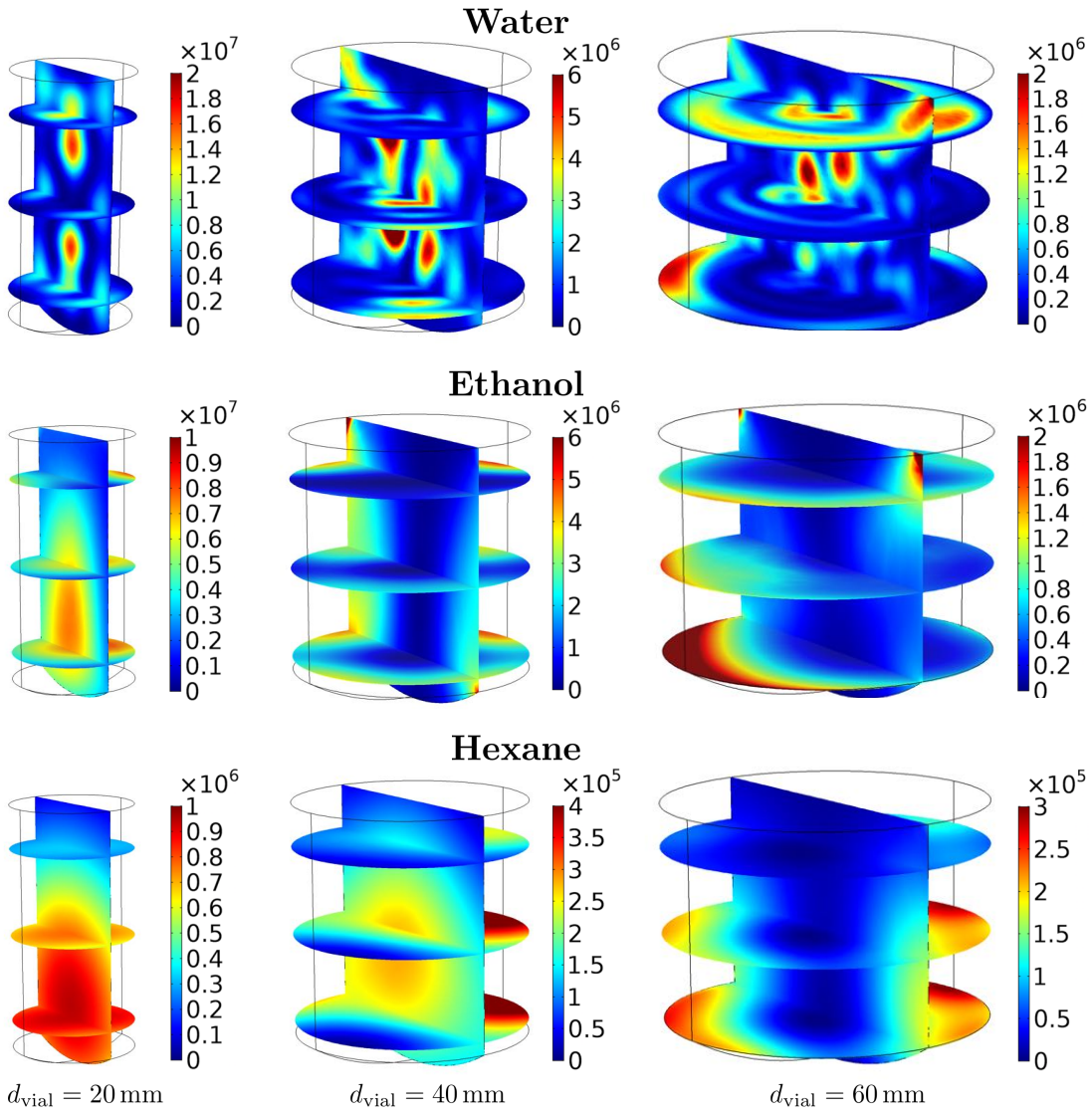

Figure 10. *Volumetric power absorbed ρ_p [W/m³] inside water (row 1), ethanol (row 2), and hexane (row 3) with a liquid height of 40 mm during scale-up. d_{vial}=20 mm (column 1), d_{vial}=40 mm (column 2), and d_{vial}=60 mm (column 3). The three disks and vertical plane show cuts from the 3D calculations.*

The penetration depth is defined as the distance at which the power of the EM field decreases to 1/e (~37%) of its incident value in a semi-infinite slab. D_p is calculated as[33]:

$$D_p = \frac{c}{2\pi f(2\varepsilon')^{1/2}} \left[\left[1 + tan^2\delta \right]^{\frac{1}{2}} - 1 \right]^{-1/2}, \qquad (12)$$

where c is the speed of light in vacuum. Using Eq. (12), D_p for water, ethanol, and hexane at 20 ^{o}C is calculated to be 16.4 mm, 8.7 mm, and 710.2 mm, respectively. In the literature, it has been suggested that the maximum diameter of the load should be smaller than $2D_p$ to achieve uniform microwave heating. However, Figure 10 clearly shows that in the case of water, even for d_{vial} = 60 mm~$4D_p$, the specific power absorbed peaks near the center of the vial. In contrast, for ethanol and hexane the maximum specific power absorbed is close to the wall for d_{vial} = 60 mm. Therefore, there is no clear correlation between D_p and the distribution of the absorbed power. It is possible that the role of penetration depth becomes important when the vial diameter is much larger than the penetration depth.

The reflection coefficient Γ is the complex ratio of the reflected wave to the incident wave and quantifies the reflection of EM waves from an interface. Γ is calculated as[23]:

$$\Gamma = \frac{\zeta_2 - \zeta_1}{\zeta_2 + \zeta_1}, \qquad (13)$$

where ζ_1 and ζ_2 are the intrinsic impedance of materials 1 and 2, respectively; microwaves travel from material 1 (water, ethanol, or hexane) to material 2 (vial). ζ_i of the i^{th} material is calculated as $\zeta_i = j\omega\mu_i/k_i$. Using Eq. (13), the magnitude of Γ for water, ethanol, and hexane in a Pyrex vial is 0.66, 0.32, and 0.14, respectively. Thus, the internal reflection of microwaves is maximum for water, followed by ethanol and hexane. The large value of Γ in the case of water points to the high internal reflection of EM waves and thus a stronger wave pattern formation observed within the sample, as shown in Figure 10.

Considering the values of D_p and Γ, there is no clear correlation between the heating non-uniformity and D_p. However, Γ seems to be playing an important role for the observed wave patterns within the vials.

It should be noted that two main ISM frequencies are available for the application of microwave heating: 2.45 GHz and 915 MHz. A frequency of 2.45 GHz is commonly used in lab-scale microwave reactors, whereas for industrial applications, a frequency of 915 MHz may be more favorable as it provides a higher penetration depth. The present work focuses on 2.45 GHz. Since the dielectric properties, reflection coefficient, and the electromagnetic field distribution in the cavity also depend on the microwave frequency, future scale-up studies should also consider the effect of frequency.

6. Conclusions

In this work, we developed a predictive computational model for a commonly used bench-scale microwave reactor (CEM Discover® SP) and explored its scale-up. A calibration curve was first developed relating the delivered microwave power to the set point power. It was found that estimation of dielectric properties and knowledge of the delivered power can render microwave models accurate, i.e., the lack of quantitative predictions of previous models is not related with the governing equations and physics of the problem, but rather to the manufacturing and knowledge of the settings of these devices.

For the scale-up study, we focused on the volumetric power absorbed, energy efficiency, and uniformity of power absorbed. During the scale-up, the power absorbed first increases, and then decreases sharply and eventually more gradually. Significant power is absorbed only for relatively small diameters for strongly microwave absorbing liquids. The energy efficiency exhibits a

strongly nonlinear response. Even though high energy efficiencies over 90% occur for microwave absorbing liquids for larger diameters, the power absorbed is low. Moreover, when the vial size becomes much larger than the penetration depth, most of the heat is generated in a narrow region close to the vial surface, making the distribution of heat less uniform.

Overall, the non-uniformity of the power absorbed underscores the need for improved microwave designs. Accurate simulation tools and detailed experiments are imperative for scale-up as no general design criteria exist for microwave-assisted chemical technologies. More work is required especially towards the development of simple models that can readily be solved to evaluate the performance of the reactor for different operating conditions at different scales.

7. Supporting Information

The Supporting Information is available free of charge on the ACS publications website. Experimental temperature profiles for microwave heating of water, ethanol, and hexane. Response surfaces for the average heating rates used in the optimization study.

8. Author Information

Corresponding Author

*Email: vlachos@udel.edu

9. Acknowledgements

This work was supported by the RAPID manufacturing institute, supported by the Department of Energy (DOE), award number DE-EE0007888-8.3. The Delaware Energy Institute is grateful to the State of Delaware for its support of the RAPID institute projects. The authors thank Dr. Sunitha Sadula for her help with the microwave heating experiments. This paper is dedicated to Christos Georgakis.

10. References

1. Chu, S.; Majumdar, A., Opportunities and challenges for a sustainable energy future. *nature* **2012,** *488* (7411), 294.
2. Adanez, J.; Abad, A.; Garcia-Labiano, F.; Gayan, P.; Luis, F., Progress in chemical-looping combustion and reforming technologies. *Progress in energy and combustion science* **2012,** *38* (2), 215-282.
3. Robinson, J.; Kingman, S.; Irvine, D.; Licence, P.; Smith, A.; Dimitrakis, G.; Obermayer, D.; Kappe, C. O., Electromagnetic simulations of microwave heating experiments using reaction vessels made out of silicon carbide. *Physical Chemistry Chemical Physics* **2010,** *12* (36), 10793-10800.
4. Musho, T. D.; Wildfire, C.; Houlihan, N. M.; Sabolsky, E. M.; Shekhawat, D., Study of Cu2O particle morphology on microwave field enhancement. *Materials Chemistry and Physics* **2018,** *216*, 278-284.
5. Gao, X.; Liu, X.; Yan, P.; Li, X.; Li, H., Numerical analysis and optimization of the microwave inductive heating performance of water film. *International Journal of Heat and Mass Transfer* **2019,** *139*, 17-30.
6. Li, H.; Meng, Y.; Shu, D.; Zhao, Z.; Yang, Y.; Zhang, J.; Li, X.; Fan, X.; Gao, X., Breaking the equilibrium at the interface: microwave-assisted reactive distillation (MARD). *Reaction Chemistry & Engineering* **2019,** *4* (4), 688-694.
7. Li, H.; Liu, J.; Li, X.; Gao, X., Microwave-induced polar/nonpolar mixture separation performance in a film evaporation process. *AIChE Journal* **2019,** *65* (2), 745-754.
8. Hayden, S.; Studentschnig, A. F. H.; Schober, S.; Kappe, C. O., A critical investigation on the occurrence of microwave effects in emulsion polymerizations. *Macromolecular Chemistry and Physics* **2014,** *215* (23), 2318-2326.
9. Kappe, C. O.; Pieber, B.; Dallinger, D., Microwave effects in organic synthesis: myth or reality? *Angewandte Chemie International Edition* **2013,** *52* (4), 1088-1094.
10. Kappe, C. O., Unraveling the mysteries of microwave chemistry using silicon carbide reactor technology. *Accounts of chemical research* **2013,** *46* (7), 1579-1587.
11. Motasemi, F.; Afzal, M. T., A review on the microwave-assisted pyrolysis technique. *Renewable and Sustainable Energy Reviews* **2013,** *28*, 317-330.

12. Parvez, A. M.; Wu, T.; Afzal, M. T.; Mareta, S.; He, T.; Zhai, M., Conventional and microwave-assisted pyrolysis of gumwood: A comparison study using thermodynamic evaluation and hydrogen production. *Fuel processing technology* **2019,** *184*, 1-11.
13. Horikoshi, S.; Kamata, M.; Serpone, N., Energy Savings through Microwave Selective Heating of Pd/AC Catalyst Particulates in a Fixed-Bed Reactor. *Chemical Engineering & Technology* **2016,** *39* (8), 1575-1577.
14. Horikoshi, S.; Kamata, M.; Sumi, T.; Serpone, N., Selective heating of Pd/AC catalyst in heterogeneous systems for the microwave-assisted continuous hydrogen evolution from organic hydrides: Temperature distribution in the fixed-bed reactor. *International Journal of Hydrogen Energy* **2016,** *41* (28), 12029-12037.
15. Sturm, G. S. J.; Verweij, M. D.; Stankiewicz, A. I.; Stefanidis, G. D., Microwaves and microreactors: design challenges and remedies. *Chemical Engineering Journal* **2014,** *243*, 147-158.
16. CEM Discover SP http://cem.com/discover-sp.
17. Sturm, G. S. J.; Verweij, M. D.; Van Gerven, T.; Stankiewicz, A. I.; Stefanidis, G. D., On the effect of resonant microwave fields on temperature distribution in time and space. *International Journal of Heat and Mass Transfer* **2012,** *55* (13-14), 3800-3811.
18. Robinson, J.; Kingman, S.; Irvine, D.; Licence, P.; Smith, A.; Dimitrakis, G.; Obermayer, D.; Kappe, C. O., Understanding microwave heating effects in single mode type cavities—theory and experiment. *Physical Chemistry Chemical Physics* **2010,** *12* (18), 4750-4758.
19. Sturm, G. S. J.; Verweij, M. D.; Van Gerven, T.; Stankiewicz, A. I.; Stefanidis, G. D., On the parametric sensitivity of heat generation by resonant microwave fields in process fluids. *International Journal of Heat and Mass Transfer* **2013,** *57* (1), 375-388.
20. Cherbański, R.; Rudniak, L., Modelling of microwave heating of water in a monomode applicator–Influence of operating conditions. *International Journal of Thermal Sciences* **2013,** *74*, 214-229.
21. Bermúdez, J. M.; Beneroso, D.; Rey-Raap, N.; Arenillas, A.; Menéndez, J. A., Energy consumption estimation in the scaling-up of microwave heating processes. *Chemical Engineering and Processing: Process Intensification* **2015,** *95*, 1-8.
22. Pianroj, Y.; Jumrat, S.; Werapun, W.; Karrila, S.; Tongurai, C., Scaled-up reactor for microwave induced pyrolysis of oil palm shell. *Chemical Engineering and Processing: Process Intensification* **2016,** *106*, 42-49.
23. Pozar, D. M., *Microwave engineering*. John Wiley & Sons: 2009.
24. COMSOL Multiphysics v. 5.3, COMSOL AB, Stock- holm, Sweden.
25. Lee, W.H., Development of microreactor setups for microwave organic synthesis. **2015**.
26. ITACA https://itacadimas.wordpress.com.
27. Kappe, C. O.; Dallinger, D.; Murphree, S. S., Practical microwave synthesis for organic chemists. *Strategies, Instruments, and Protocols (Wiley-VCH, Weinheim, Germany, 2009)* **2009**.
28. Catalá-Civera, J. M.; Canós, A. J.; Plaza-González, P.; Gutiérrez, J. D.; García-Baños, B.; Peñaranda-Foix, F. L., Dynamic measurement of dielectric properties of materials at high temperature during microwave heating in a dual mode cylindrical cavity. *IEEE transactions on microwave theory and techniques* **2015,** *63* (9), 2905-2914.
29. Dimitrakis, G. A.; George, M.; Poliakoff, M.; Harrison, I.; Robinson, J.; Kingman, S.; Lester, E.; Gregory, A. P.; Lees, K., A system for traceable measurement of the microwave

complex permittivity of liquids at high pressures and temperatures. *Measurement Science and Technology* **2009,** *20* (4), 045901.
30. Goyal, H.; Pepiot, P., On the validation of a one-dimensional biomass pyrolysis model using uncertainty quantification. *ACS Sustainable Chemistry & Engineering* **2018,** *6* (9), 12153-12165.
31. Box, G. E. P.; Hunter, W. G.; Hunter, J. S., Statistics for experimenters. **1978**.
32. Ayappa, K. G.; Davis, H. T.; Crapiste, G.; Davis, E. A.; Gordon, J., Microwave heating: an evaluation of power formulations. *Chemical engineering science* **1991,** *46* (4), 1005-1016.
33. Metaxas, A. C. a.; Meredith, R. J., *Industrial microwave heating*. IET: 1983.

TOC/ Abstract Graphic